KOM
CORROSION AND MATERIAL PROTECTION JOURNAL

ORIGINAL ARTICLE

sciendo

Experimental studies on the corrosion inhibition of mild steel by 1-(phenylamino--1,3,4-thiadiazol-5-yl)-3-phenyl-3-oxopropan complemented with DFT Modeling

Alamiery A.[1,2] *, Ali J.M.*[1]*, Isahak W.N.R.*[1]

[1] **Department of Chemical and Process Engineering, Faculty of Engineering and Built Environment, University Kebangsaan Malaysia (UKM), Bangi, Selangor, Malaysia**

[2] **University of Technology (UOT), Baghdad, Iraq**

E-mail: dr.ahmed1975@ukm.edu.my

1-(Phenylamino-1,3,4-thiadiazol-5-yl)-3-phenyl-3-oxopropan (PTPO) was selected as the investigated material for studying the protection performance for mild steel in 1 mol L-1 hydrochloric acid solution. The inhibitor was assessed using weight loss measurements complemented with morphological analytical techniques and density functional theory (DFT) modelling. The PTPO demonstrated significant inhibitive efficacy of 95.4% in the presence of 500 ppm at 303 K. The protection efficiency increases with the concentration increasing from 100 to 500 ppm, and no significant effect after 500 ppm. Furthermore, gravimetric findings reveal that the protection efficiency at 500 ppm PTPO increases with immersion period and increasing temperature (303-333 K), due to the effective adsorption of PTPO on the mild steel surface, and the protection efficiency value is 95.8% at 48 h of exposure and 95.4%, 95.4%, 95.7% and 95.9% at 303, 313, 323 and 333 K, respectively. The adsorption of PTPO on the mild steel surface obeyed the Langmuir adsorption isotherm model and revealing the mode of chemisorption adsorption. According to the DFT calculations, protection by PTPO is essentially performed by the heteroatoms in the inhibitor molecules which represented the adsorption sites, and the aromatic rings increase the electrostatic interaction between the PTPO molecules and the mild steel surface. The surface morphological studies, weight loss measurements, and DFT computational studies are in good agreement and that the selected corrosion inhibitor is adsorbed on the mild steel surface to form a protected layer on the surface of mild steel against the hydrochloric acid solution.

INTRODUCTION

The investigation of methods to avoid metal corrosion is an essential problem in the subject of corrosion that necessitates scientists to focus on research. Metal corrosion can be retarded and prevented in a variety of ways, including designing materials to avoid corrosion, selecting appropriate materials for each environment, protecting surfaces with coatings, electrochemical treatments, and so on. Corrosion inhibitors, in particular, are employed as a low-cost, high-efficiency method [1]. Adsorption and the development of a coating on the metal surface are used by inhibitors to carry out their functions. As a result, they prevent corrosion by increasing anode or cathode polarisation, restricting ion migration or diffusion onto the metal surface, and improving metal surface resistance [2]. In addition, mild steel is low natural stability and is profoundly degraded in the mineral acid environment such as HCl, H_2SO_4, HNO_3. Various industries and operations, i.e., acid pickling, oil industry, oil-well, and heat exchangers cleaning processes utilize highly acidic media particularly HCl solutions. The acidic conditions could deleteriously affect the surface and may decrease the service life of the equipment. Therefore, precise control and monitoring of the corrosion processes are always required. In acid solutions, organic compounds containing phosphorous, sulphur, oxygen, and/or nitrogen atoms have been tested as effective corrosion inhibitors for steel [3-5]. Furthermore, the presence of benzene rings in the inhibitor molecule is a significant component because it boosts the inhibitor-metal surface electrostatic interaction [6]. As a result, it improves metal inhibition over a longer period of time. Organic compounds containing both heteroatoms and benzene rings are thus attractive possibilities to explore when looking for potential corrosion inhibitors. Mild steel is a common iron alloy with a wide range of industrial applications. Mild steel‘s popularity as a construction material and other applications can be ascribed to its inexpensive cost and high mechanical strength [7]. Mild steel, on the other hand, is easily corroded in everyday situations. Acid solutions, particularly hydrochloric acid, are typically very aggressive media for mild steel corrosion. They are employed in various industrial operations such as acid cleaning, oil-well acidizing, acid descaling, and so on [8]. Due to the molecule of 1-(phenylamino-1,3,4-thiadiazol-5-yl)-3-phenyl-3-oxopropan (PTPO) contains nit-

rogen, oxygen, and sulphur heteroatoms as well as benzene rings, it can transfer its electrons into unoccupied d-orbitals of iron atoms on the surface of mild steel to produce a strong metal-protective coating by coordinate bonding. As a result, PTPO has the potential to be a corrosion inhibitor in hydrochloric acid environments. Other corrosion inhibitors with differing nitrogen, oxygen, and sulfur atoms are also considered for comparison purposes in order to assess the influence of heteroatoms on steel corrosion inhibition [9-22]. We wish to look into the impact of immersion time and solution temperature on corrosion inhibition mechanisms in this study. The experimental results were explained in depth using theoretical calculations. Quantum chemical calculations were used to create a correlation between molecular structure and corrosion inhibition performance in order to achieve this goal. As a result, the current work looks into PTPO adsorption on mild steel in a 1 mol L^{-1} hydrochloric acid environment. The goal was to compare the corrosion inhibition potential of PTPO to that of other produced corrosion inhibitors in order to see how substituent groups affected PTPO‘s corrosion inhibition property (Table 1). The weight-loss method was used to test the PTPO‘s inhibitive ability on mild steel corrosion in 1 1 mol L^{-1} HCl. To provide theoretically based reasons for the inhibitive behaviour of the investigated PTPO, quantum chemical simulations were performed. The novelty of the present study is to synthesize a new inexpensive, non-toxic, and eco-friendly 1,3,4-thiadiazol derivative and investigate its efficiency as a corrosion inhibitor for mild steel in 1 mol L^{-1} hydrochloric acidic media using mass loss techniques. Furthermore, this study aimed to understand the relationship between the molecular structure of this inhibitor and its inhibitive action.

EXPERIMENTAL DETAILS

Materials and reagents

The chemicals were purchase from Sigma-Aldrich and used without further purification. The tested inhibitor was synthesized according to the general procedure Abu-Husham [33]. The yield 69% as a yellowish solid and the melting points 285 °C ([33], 283-285 °C). PTPO is used as a corrosion inhibitor in the current investigation. The chemical structure of PTPO is shown in Figure 1.

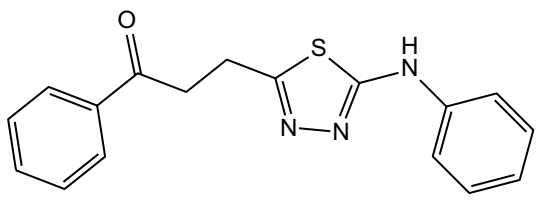


Fig. 1. The chemical structure of PTPO

Acidic solution

Diluting the analytical grade of hydrochloric acid with distilled water yielded the acidic solution (blank solution) of 1 mol L^{-1} HCl. The inhibitor concentrations were 100, 200, 300, 400, 500, and 1000 ppm.

Weight loss measurements

The rate of corrosion and inhibition efficiency due to the protection of PTPO was evaluated by weight loss measurements using the ASTM technique G01-03 [34]. The mirror-like coupons were cleaned in a sonicating acetone bath for 30 minutes, soaked in ethanol, and dried in the oven before being exposed to a corrosive environment. After that, the weight of the coupon was measured before it was exposed to PTPO. After being exposed to various concentrations of PTPO for 1, 5, 10, 24, and 48 hours, the coupons were removed, rinsed with distilled water, soaked with acetone, and dried in the oven [35]. The weight loss analysis was conducted in triplicates and average mass loss was calculated in every experiment to guarantee reproducibility. The rate of corrosion was determined according to Equation (1):

$$C_R = \frac{\Delta W}{at} \tag{1}$$

where C_R is the rate of corrosion (g/(cm^2. h); ΔW represents the mild steel coupons average weight loss (g); a is the mild steel coupon surface area (cm^2) and t is the immersion time (h).

From the determined values of corrosion rates, the protection efficiency (% IE) was calculated according to Equation (2) [36]:

$$IE = \frac{C_{R1} - C_{R2}}{C_{R1}} \times 100 \tag{2}$$

where C_{R1} is the value of corrosion rate in the absence of PTPO whereas the C_{R2} represents the values of corrosion rate in the various concentrations of PTPO.

DFT investigation

DFT (density functional theory) calculations we conducted using the Gaussian 03 program [37]. The structure of the tested inhibitor was first optimized at B3LYP/6-311G(d,p).

We used in our calculation, the DFT (Density Functional Theory) method of the three-parameter compound of Becke (B3LYP). One of the most commonly used versions is B3LYP, which stands for „Becke, 3-parameter, Lee–Yang–Parr“. The 6-311G(d,p) basis set was used for all calculations. The „6-31G“ is the standard, split-valence double-zeta basis set, the functions you will use to describe your core and valence orbitals. Functions in parentheses „(d)“ or „(d,p)“ are polarization functions,

those used to properly describe chemical bonds (higher angular momentum than the valence orbitals). If there is no comma, such as „(d)“ or it means that you are including polarization functions in all „heavy“ atoms. Functions identified with „+“ are diffuse functions, „++“ means diffuse functions for all atoms.

According to the DFT calculations, the quantum chemical parameters such as the frontier molecular orbitals (HOMO and LUMO energy levels), energy gap (ΔE), electronegativity (χ), hardness (η), softness (σ), dipole moment (μ), number of transferred electron (ΔN) and Mulliken charges were conducted [38-40].

$$\Delta E = E_{\text{HOMO}} - E_{\text{LUMO}} \tag{3}$$

$$\eta = \frac{E_{\text{HOMO}} - E_{\text{LUMO}}}{2} \tag{4}$$

$$\sigma = \frac{1}{\eta} \tag{5}$$

$$\chi = \frac{E_{\text{HOMO}} + E_{\text{LUMO}}}{2} \tag{6}$$

$$\Delta N = \frac{\chi_{\text{Fe}} - \chi_{\text{inh}}}{2(\eta_{\text{Fe}} + \eta_{\text{inh}})} \tag{7}$$

where χ_{Fe} and η_{Fe} were 7 eV mol^{-1} and 0 eV mol^{-1}, respectively.

RESULTS AND DISCUSSION

Concentration effect

The corrosion rate and protection efficiency of the inhibitor PTPO at various concentrations (100, 200, 300, 400, 500 and 1000 ppm) and different temperatures (303, 313, 323 and 333 K) were evaluated by gravimetrical techniques, and the results are demonstrated in Figures 2 and 3. The protection efficiency increased on increasing the PTPO concentration, and a decrease in the corrosion rate was shown at all studied concentrations, as illustrated in Figure 2. Hence, it is obvious that the protection efficiency was concentration-dependent. With increasing PTPO concentration, considerable PTPO molecules numbers are adsorbed on the tested coupon surface, which appears in increased protection performance. The adsorbed inhibitor molecules control and/or block the reaction sites and hence protect the coupon surface from corrosive solution. While the PTPO has significant ion pairs of electrons, such as ion pairs on sulphur, oxygen, and nitrogen atoms, and the pi-electrons, that are coordinately bonded with iron atoms on the coupon surface, they could retard corrosion. For the inhibitor concentration of 500 ppm and 303 K and immersion time of 5 hours, PTPO exhibited the highest protection efficiency of 95.4 %. Behind that, no significant improvement in protection efficiency was recognized with additional increases in PTPO concentration. As we have seen from Figure 2, for the inhibitor concentration of 1000 ppm highest inhibition efficiency was 95.9 %.

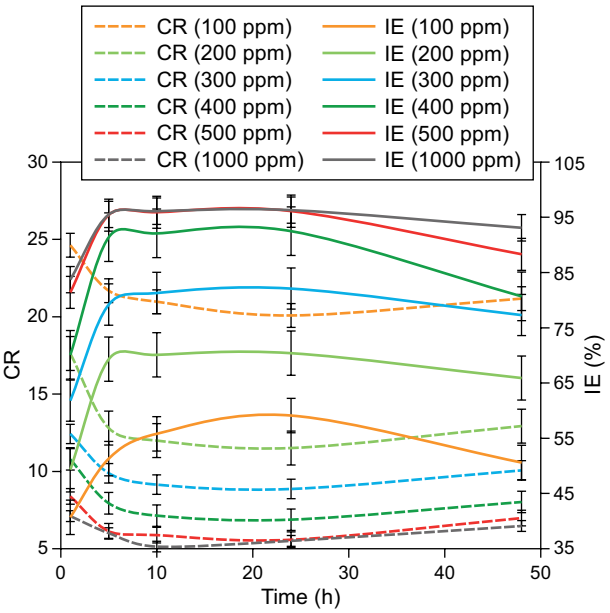


Fig. 2. Corrosion rate and inhibition efficiency obtained from weight loss techniques for mild steel in 1 mol L^{-1} HCl at various immersion periods and different concentrations of PTPO at 303 K

Figure 2 above exhibits the difference of the corrosion rates and inhibitor efficiencies with the immersion time (h) shown for the mild steel in 1.0M HCl medium with different concentrations of PTPO as a corrosion inhibitor. The effect of time on the rates of corrosion values for various inhibitor concentrations (100-1000 ppm) at 303 K is exhibited in Figure 2. The corrosion rate was recognized to decrease as the exposure period and concentration of PTPO increases. In presence of 100 ppm of PTPO, an increase of corrosion rate from 20.08-21.17 mm/y was recognized for the immersion time from 24-48 h. The experimental findings achieved confirm that exposure time has an important impact on mass loss, rate of corrosion, protection efficacy, and surface coverage degree (IE/100). The experimental findings as in Figures 2 revealed that the rate of corrosion increase with the exposure period for the tested coupons and at all the studied concentrations of tested inhibitors. However, when analysing the mass lost values for the mild steel coupons, the untreated coupons (in absence of tested inhibitor) recorded the highest corrosion rate 73.24 mm/y, while the corrosion rate for the inhibited coupons (in presence of tested inhibitor) recorded decreased overall with an increase in inhibitor concentration. After 24 h of exposure period in presence of the tested inhibitor, the corrosion rate increase slightly. Thus,

the slight increase in corrosion could be attributed to the increased immersion time in the acidic solution. Figure 2 shows a plot of the corrosion rate with inhibition efficiency (%) versus time (hours) for various inhibitor concentrations. From these results, it can be seen that the inhibition efficiency increased with increasing time significantly for all levels of inhibitor concentration. Then, a decrease in the value was observed after 24 hours and depending on the concentration of the inhibitor.

Temperature effect

Temperature highly affects the corrosion rate and the inhibition efficiency, and with increasing temperature, the rate of corrosion increases exponentially in an acidic environment [41-45]. To understand the protection performance of the tested inhibitor at various temperature degrees, 303–333 K, the corrosion rate and inhibition efficiency were investigated. The tested inhibitor revealed the highest inhibition efficiency at 303 K, which regularly declined with an increase in temperature. The tested inhibitor exhibited lower protection performance at maximum temperature. This results attending to the fact that the temperature rise did not support physisorption (physical interactions), therefore reducing the protection performance. Figure 3 reveals that when the temperature rises, the protection efficiency of PTPO decrease. Particularly, the protection efficiency of PTPO reduces from 95.4 to 78.5 % and that of when the temperature varies in the domain of 303-333 K at the concentration of 500 ppm. These findings attributed to that the molecules of PTPO are separated from the mild steel surface, the metal is no longer protected, and so the inhibitive efficiency decrease as the temperature increases.

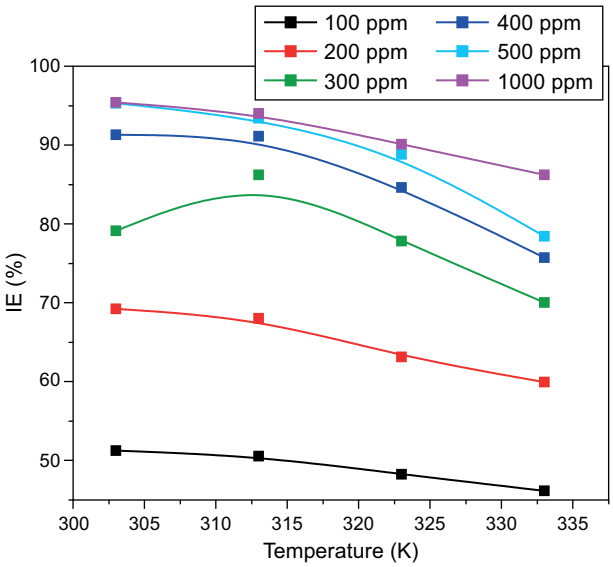


Fig. 3. Inhibition efficiency obtained from weight loss techniques for mild steel in 1 mol L^{-1} HCl at various temperatures and different inhibitor concentrations

As noted from Table 1, the investigated compound PTPO has significant inhibitive performance as compared with other synthesized inhibitors in addition to the easily synthesis one shot. The corrosion inhibitors shown in Table 1 had proportionally lower or equal protection performance compared to the studied inhibitor, as well as being expensive to synthesise, with reactions requiring more than one step and requiring expensive solvents.

Adsorption isotherms

Adsorption isotherms derived from chemisorption or physisorption were used to investigate the interaction between corrosion inhibitor molecules and mild steel surface. The degree of surface coverage of the inhibitor molecules has a major impact on the corrosion. As a result, the inhibition efficiency is defined as a function of the surface covered by inhibitor molecules [41]. The linear

Tab. 1. Published corrosion inhibitors compared to the studied one

Inhibitors	Protection performance	Reference
1-(Phenylamino-1,3,4-thiadiazol-5-yl)-3-phenyl-3-oxopropan (PTPO)	95.4 %	Current Investigation
4-benzyl-1-(4-oxo- 4-phenylbutanoyl)thiosemicarbazide (BOT)	92.5 %	23
N‘-(2-(2- oxomethylpyrrol-1-yl)ethyl)piperidine	91.9%	24
2-N-phenylamino-5-(3-phenyl-3-oxo-1-propyl)-1,3,4-oxadiazole	95.1%	25
2-Amino-4-phenyl-N-benzylidene-5-(1,2,4-triazol-1-yl)thiazole (APNT)	98.1%	26
N‘-(2-hydroxybenzylidene)-2-(quinolin-8-yloxy)acetohydrazide (NHQA)	93.0 %	27
2- ((6-Methyl-2-Ketoquinolin-3-yl)Methylene) Hydrazinecarbothioamide	95.8%	28
terephthalo- hydrazide	96.4 %	29
5-((4-fluoro-benzylidene)amino)-1,3,4-thiadiazole-2-thiol (FATT)	91.0 %	30
4-pyrrol-1-yl-N-(2,5-dimethylpyrrol-1-yl)benzoylamine	95.8 %	31
N´-(1-phenylethylidene)-4-(1H-pyrrol-1-yl)benzohydrazide (N–PB)	96.0 %	32

relationship of the adsorption isotherm was determined using the concentration and degree of surface covering. For a better understanding of the behaviour of the tested inhibitor, various adsorption isotherms such as Frumkin, Temkin, and Langmuir were investigated, with the Langmuir isotherm model being the best fit. Equation (8) was used to show the link between the degree of surface covering (θ) and concentration as in Equation (9).

$$\frac{C}{\theta} = \frac{1}{K_{ads}} + C \tag{8}$$

$$\theta = \frac{IE}{100} \tag{9}$$

where K_{ads} is the constant of equilibrium.

While a plot was outlined between concentration and concentration/θ, a straight line with a slope of one and coefficient of regression of 0.998 was achieved, as revealed in Figure 4. The linear relation suggests that the inhibitor molecules adsorbed on the surface of mild steel followed the Langmuir isotherm model [42,43]. The equilibrium constant was calculated according to Equation (8), and the adsorption free energy was determined from the value of the equilibrium constant based on Equation (10).

$$\Delta G^{\circ}_{ads} = -RT \ln (55.5\, K_{ads}) \tag{10}$$

where T signifies the temperature, R is the constant of gas, and 55.5 mol dm^{-3} is the water concentration.

ΔG°_{ads} determined applying Equation (10) was 36.38 kj mol^{-1}. This value implied that the adsorption of inhibitor molecules on the mild steel surface was a spontaneous process. It has previously been observed that lower negative ΔG°_{ads} value (20.00 kj mol^{-1}) imply adsorption mostly owing to physisorption (electrostatic interactions), while higher negative ΔG°_{ads} value (24.00 kj mol^{-1}) indicate chemisorption (chemical reaction through the formation of coordination bonds between the pairs of electrons of heteroatoms of tested inhibitor molecules and d-orbitals of iron atoms on the mild steel surface) [32]. The value of ΔG°_{ads} in this investigation, indicating that the form of adsorption is chemisorption.

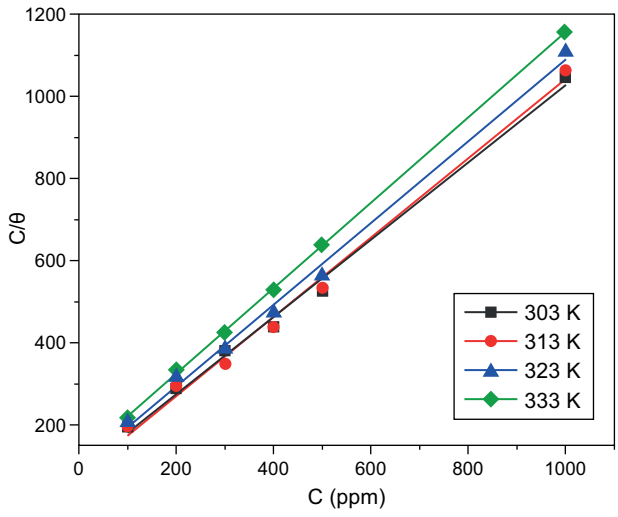


Fig. 4. Langmuir adsorption isotherm model for the tested inhibitor molecules on the surface of mild steel in 1 mol L^{-1} HCl at various temperatures

Theoretical Calculations

Optimized structure, EHOMO, ELUMO of PTPO at B3LYP/6-311G(d,p) are presented in Figure 5. The energies of the highest occupied molecular orbital and lowest unoccupied molecular orbital can present the donating and accepting electron positions of the PTPO molecule [44-46]. Figure 5, represents the optimized, HOMO and LUMO structures of PTPO. PTPO (O and N atoms) tends to donate electrons to the d-orbital of iron atoms on the mild steel surface and form coordination bonds. LUMO indicates that some sites in PTPO molecules have the ability to receive electrons from iron atoms.

E_{HOMO} energy, E_{LUMO}, ΔE, χ, η, and σ are calculated for PTPO as Quantum chemical parameters in Table 2.

The energy gap is a significant descriptor, which symbolizes the adsorption of inhibitor molecules toward the mild steel surface [47]. The organic molecule which has an energy gap with a low value is usually described by excellent protection efficiency. Moreover, the values

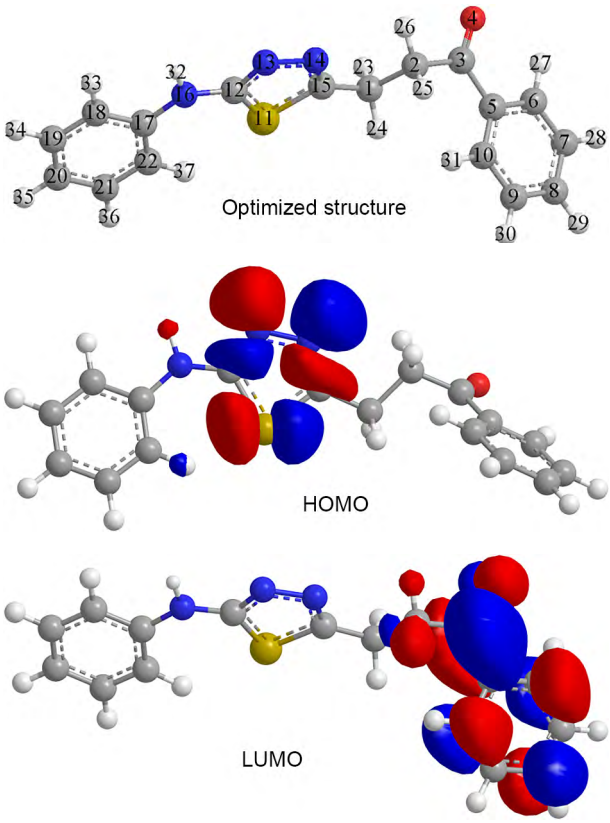


Fig. 5. Optimized structure, HOMO, and LUMO of PTPO molecule

Tab. 2. Quantum Chemical Parameters of PTPO at B3LYP/6-311G(d,p)

E_{HOMO} (eV)	E_{LUMO} (eV)	ΔE (eV)	χ (eV)	η (eV)	σ (eV^{-1})	ΔN
-8.984	–5.046	3.938	7.015	1.969	0.507	-0.0038

of η, S, and ΔN in Table 2 show that PTPO has the ability to control and or retard the mild steel surface from corrosive solution. That is in excellent agreement with the laboratory findings of protection efficiency. When compared to other inhibitors with lower hardness values, inhibitors with high hardness (η) values are likely to be weaker [48]. The hardness value increases as the percent IE increases. As can be seen in Table 2, the tested inhibitor has a significant value (1.969 eV), indicating that the investigated compound can be an inhibitor for corrosion of mild steel in hydrochloric acid solution, which is consistent with the experimental result in Figure 2 (IE = 95.8 %). The higher value of σ reveals that the tested inhibitor has a soft nature and donats electrons to the iron atoms on the surface of mild steel [49]. This indicates that the examined inhibitor molecule has the maximum inhibitory efficacy and, as a result, is the most reactive inhibitor molecule. From Table 2, it can be seen that the value of χ for the tested inhibitor is 7.015 eV, therefore, it is proved that the tested inhibitor has the significant ability to accept electrons and this result is in excellent harmony with the experimental results. The ΔN value demonstrates the fraction of electrons that transfer from the inhibitor molecules to the unoccupied d-orbital of iron atoms on the mild steel surface. If $\Delta N > 0$, then electrons were transferred from the inhibitor molecule to unoccupied d-orbital of iron atoms on the mild steel surface, on the second hand if $\Delta N < 0$, then electrons were transferred from metal to inhibitor molecules through back-donation mechanism [50]. From Table 2, it can be seen that the ΔN value of the examined inhibitor is less than 0, this confirms that the electrons were transferred from iron atoms on a mild steel surface to inhibitor molecules through a back-donation mechanism. Analysis of these findings in Table 2 proves the ability to donate electrons as observed from its experimental results.

The mechanism of inhibition can be determined via adsorption studies depending on weight loss methods and also theoretical calculations. Computational chemistry, such as quantum chemical simulations, has lately been applied to understand the process of corrosion inhibition [51]. Quantum chemical computations have been shown to be an extremely effective technique for investigating mechanisms [52]. The goal of this research is to present a theoretical investigation of PTPO's electronic and molecular structure (Figure 5) and to explore the relation between PTPO's molecular structure and inhibitory efficiency. The basic parameters, such as HOMO and LUMO, the atomic charge of the studied inhibitor, the absolute electronegativity (χ), hardness (η), softness (σ), dipole moment (μ) values, and the fraction of electrons (ΔN) transfer from PTPO molecules to mild steel were also determined.

Based on published studies [53, 54], the ΔN value revealed that the protection performance produced from the donation of electrons. According to Lukovits's investigation [54], if ΔN is less than 3.6, the protection performance increased with increasing the ability to donate electrons at the mild steel surface. In the current investigation, the PTPO molecules were the electrons donator, and the Fe atoms on the mild steel surface were the acceptors. The PTPO molecules were bound to the Fe atoms on the mild steel surface and hence produced a protection adsorption layer versus corrosive solution. PTPO molecules had significant protection performance due to high EHOMO and ΔN value, and it had the good ability to offer electrons. Based on published studies [53, 54], the ΔN value revealed that the protection performance produced from the donation of electrons. According to Lukovits's investigation [54], if ΔN is less than 3.6, the protection performance increased with increasing the ability to donate electrons at the mild steel surface. In the current investigation, the PTPO molecules were the electrons donator, and the Fe atoms on the mild steel surface were the acceptors. The PTPO molecules were bound to the Fe atoms on the mild steel surface and hence produced a protection adsorption layer versus corrosive solution. PTPO molecules had significant protection performance due to high EHOMO and ΔN value, and it had the good ability to offer electrons.

Tab. 3. Mulliken Charges of PTPO

atoms	C(1)	C(2)	C(3)	O(4)	C(5)	C(6)	C(7)	C(8)
charges	-0.439319	-0.441811	0.42906	-0.456293	-0.078277	-0.153731	-0.185191	–0.1
atoms	C(9)	C(10)	S(11)	C(12)	N(13)	N(14)	C(15)	N(16)
charges	-0.180666	-0.205815	0.468237	0.280243	-0.351686	-0.315109	0.005621	-0.871746
atoms	C(17)	C(18)	C(19)	C(20)	C(21)	C(22)	H(23)	H(24)
charges	0.331970	-0.195173	-0.181273	-0.189696	-0.183046	-0.198328	0.247732	0.229992

Mulliken Charges

Mulliken charges are used to detect inhibitor adsorption sites [50]. The easier it is for the atoms to transfer electrons, the more negatively charged they are. Table 3 reveals that the N and O atoms in PTPO are electron-donating locations.

CONCLUSIONS

Examining mild steel corrosion protection of PTPO with weight loss techniques as in addition to quantum chemical calculations, and remarkable outcomes may be summarized as follows:

- Weight loss techniques present the protection efficiency of PTPO as 81.4 %, 95.4 %, 95.9 %, 96.1 % and 88.3 % at the concentration 500 ppm, for the immersion periods 1, 5, 10, 24 and 48 h at 303 K.
- The protection efficiency trend gained from Weight loss techniques reveals that with increasing inhibitor concentration, the protection efficiency reaches a maximum value of 95.9 % for PTPO and at 500 ppm and no significant change when increasing the inhibitor concentration to 1000 ppm.
- The protection efficiency of PTPO decreases slightly when the temperature rises. The adsorption of PTPO molecules obeys the Langmuir adsorption isotherm model.
- The value of ΔG confirms that the process of adsorption is chemisorption.
- The heteroatoms present in the PTPO molecules give the ability to inhibit mild steel corrosion coordinate with d-orbital of iron atoms on the surface of mild steel.
- Quantum chemical calculations are in excellent agreement with the results from weight loss techniques.

REFERENCES

1. M. Athar, H. Ali, M.A. Quraishi, Corrosion inhibition of carbon steel in hydrochloric acid by organic compounds containing heteroatoms, *British Corros. J.* **2002,** 37, 155–158, https://doi.org/10.1179/000705902225002376.
2. L. Guo, I.B. Obot, X. Zheng, X. Shen, Y. Qiang, S. Kaya, C. Kaya, Theoretical insight into an empirical rule about organic corrosion inhibitors containing nitrogen, oxygen, and sulfur atoms, *Appl. Surf. Sci.* **2017,** 406, 301–306, https://doi.org/10.1016/j.apsusc, **2017**, 2, 134.
3. S.K. Saha, A. Hens, N.C. Murmu, P. Banerjee, A comparative density functional theory and molecular dynamics simulation studies of the corrosion inhibitory action of two novel N-heterocyclic organic compounds along with a few others over steel surface, *J. Mol. Liq.* **2016,** 215, 486–495, https://doi.org/10.1016/j.molliq.2016.01.024.
4. C. Verma, D.K. Verma, E.E. Ebenso, M.A. Quraishi, Sulfur and phosphorus heteroatom-containing compounds as corrosion inhibitors: an overview, *Heteroatom Chem.* **29** (4) (2018) e21437, https://doi.org/10.1002/hc.21437.
5. O. Fergachi, F. Benhiba, M. Rbaa, M. Ouakki, M. Galai, R. Touir, M.E. Touhami, Corrosion inhibition of ordinary steel in 5.0 M HCl medium by benzimidazole derivatives: electrochemical, UV–visible spectrometry, and DFT calculations, *J.Bio. Tribo-Corros.* **2019**, 5, 21, https://doi.org/10.1007/s40735-018-0215-3.
6. R. Prabhu, B. Roopashree. T. Jeevananda, S. Rao, K. R. Reddy, A. V. Raghu, Synthesis and corrosion resistance properties of novel conjugated polymer-Cu2Cl4L3 composites, *Materials Science for Energy Technologies.* **2021**, 4, 92-99, https://doi.org/10.1016/j.mset.2021.01.001.
7. H. Kumar, T. Dhanda, Application of 1,2,3-Benzotriazole as corrosion inhibitor for mild steel in sulphuric acid medium at different temperature, *Asian J. Chem.* **2020**, 32, 153–160, https://doi.org/10.14233/ajchem.2020.22379.
8. D. Gopi, E.-S. Sherif, V. Manivannan, D. Rajeswari, M. Surendiran, L. Kavitha, Corrosion and corrosion inhibition of mild steel in groundwater at different temperatures by newly synthesized benzotriazole and phosphono derivatives, *Indust. Engg. Chem. Res.* **2014**, 53,4286–4294, https://doi.org/10.1021/ie4039357.
9. I. Chung, R. Malathy, R. Priyadharshinl, V. Hemapriya, S. Kim, M. Prabakaran, Inhibition of mild steel corrosion using Magnolia kobus extract in sulphuric acid medium, *Materials Today Communications* **2020**, 25, 101687, https://doi.org/10.1016/j.mtcomm.2020.101687
10. W. Chai, D.Sun, K. Cheah, G. Li, H. Meng, Co-Electrolysis-Assisted Decomposition of Hydroxylammonium Nitrate–Fuel Mixtures Using Stainless Steel–Platinum Electrodes, *ACS Omega* **2020**, 5, 19525–19532, https://doi.org/10.1021/acsomega.0c01804.
11. A. Berrissoul, A. Ouarhach, F. Benhiba, A. Romane, A. Zarrouk, A. Guenbour, B. Dikici, A. Dafali, Evaluation of *Lavandula mairei* extract as green inhibitor for mild steel corrosion in 1 M HCl solution. Experimental and theoretical approach, *Journal of Molecular Liquids* **2020**, 313, 113493, https://doi.org/10.1016/j.molliq.2020.113493.
12. F. A. Ansari,M. A. Quraishi, Oleo-chemicals triazoles as effective corrosion inhibitors for mild steel in acetic acid. Petromin. *Pipeliner* **2010**, 36−42.
13. H. Lgaz, R. Salghi, K. Subrahmanya Bhat, A. Chaouiki, Shubhalaxmi, S. Jodeh, Jodeh Correlated experimental and theoretical study on inhibition behavior of novel quinoline derivatives for the corrosion of mild steel in hydrochloric acid solution, *J. Mol. Liq.* **2017**, 244, 154–168, https://doi.org/10.1016/j.molliq.2017.08.121.
14. M. Lagrenée, B. Mernari, M. Bouanis, M. Traisnel, F. Bentiss, Study of the mechanism and inhibiting efficiency of 3,5-bis(4-methylthiophenyl)-4H-1,2,4-triazole on mild steel corrosion in acidic media, *Corros. Sci.* **2002**, 44 (3), 573–588.
15. E. Ebenso, N. Eddy, A. Odiongenyi, Corrosion inhibition and adsorption properties of methocarbamol on mild steel in acidic medium. *Port. Electrochim. Acta* **2009**, 27, 13−22.
16. A. Afidah, E. Rahim, J. Rocca, M. Steinmetz, R. Kassim, S. Ibrahim, Mangrove tannins and their flavanoid monomers as alternative steel corrosion inhibitors in acidic medium. *Corros. Sci.* **2007**, 49, 402−417.

17. L. Herrag, A. Chetouani, S. Elkadiri, B. Hammouti, A. Aouniti, Pyrazole derivatives as corrosion inhibitors for steel in hydrochloric Acid. Port. *Electrochim. Acta* **2008**, 26, 211−220
18. F. Chaouket, B. Hammouti, S. Kertit, K. Kacemi, Corrosion inhibition of three Fe-B based amorphous alloys in sulphuric acid medium by mercaptophenytetrazole. *Bull. Electrochem* **2007**, 17, 311− 320.
19. G. K. Gomma, M. H. Wahdan, Effect of copper cation on electrochemical behaviour of steel in presence of imidazole in acid medium. *Mater. Chem. Phys.* **1997**, 47, 176−183.
20. M. Lagrenee, B. Mernari, N. Chaibi, M. Traisnel, H. Vezin, F. Bentiss, Investigation of the inhibitive effect of substituted oxadiazoles on the corrosion of mild steel in HCl medium. *Corros. Sci.* **2001**, 43, 951−962.
21. A. Abu-Hashem, Synthesis and antimicrobial activity of new 1,2,4-triazole, 1,3,4-oxadiazole, 1,3,4-thiadiazole, thiopyrane, thiazolidinone, and azepine derivatives. *J Heterocyclic Chem.* **2021**,58, 74–92. https://doi.org/10.1002/jhet.414992 ABU-HASHEM
22. ASTM G1-03(2011), Standard Practice for Preparing, Cleaning, and Evaluating Corrosion Test Specimens, ASTM International, West Conshohocken, PA, **2011**, www.astm.org.
23. A. Alamiery, W. Isahak, M. Takriff, Inhibition of Mild Steel Corrosion by 4-benzyl-1-(4-oxo-4-phenylbutanoyl)thiosemicarbazide: Gravimetrical, Adsorption and Theoretical Studies. *Lubricants* **2021**, 9, 93. https://doi.org/10.3390/lubricants9090093
24. A. Alamiery, Study of Corrosion Behavior of N'-(2-(2-oxomethylpyrrol- 1-yl)ethyl)piperidine for Mild Steel in the Acid Environment. *Biointerface Research in Applied Chemistry* **2022**, 12, 3638 - 3646
25. A. Alamiery, Corrosion inhibition effect of 2-N-phenylamino-5-(3-phenyl-3-oxo-1-propyl)-1,3,4-oxadiazole on mild steel in 1 M hydrochloric acid medium: Insight from gravimetric and DFT investigations. *Materials Science for Energy Technologies* **2021**, 4, 398-406
26. A. Alamiery, A. Kadhum, A. Mohamad, M. Takriff, The synergistic role of azomethine group and triazole ring at improving the anti-corrosive performance of 2-amino-4-phenylthiazole, *South African Journal of Chemical Engineering* **2021**, 38, 41-53.
27. A. Alamiery, Investigations on Corrosion Inhibitory Effect of Newly Quinoline Derivative on Mild Steel in HCl Solution Complemented with Antibacterial Studies. *Biointerface Research in Applied Chemistry* **2022**, 2, 1561–1568.
28. M. M. Hanoon, A. M. Resen, A. A. Al-Amiery, A. A. H. Kadhum, M. S. Takriff, Theoretical and Experimental Studies on the Corrosion Inhibition Potentials of 2-((6- Methyl-2-Ketoquinolin-3-yl)Methylene) Hydrazinecarbothioamide for Mild Steel in 1 M HCl. *Prog. Color Colorants Coat.* **2022,** 15, 11-23.
29. S. Al-Baghdadi, A. Al-Amiery, T. Gaaz, A. Kadhum, Terephthalohydrazide and isophthalo-hydrazide as new corrosion inhibitors for mild steel in hydrochloric acid: Experimental and theoretical approaches, *Koroze a Ochrana Materialu* **2021**, 65(1), 12–22.
30. Eltmimi, A.J.M. Alamiery, A. Allami, A.J. Yusop, R.M. Kadhum, A.H. and Allami, T. Inhibitive effects of a novel efficient Schiff base on mild steel in hydrochloric acid environment. *Int. J. Corros. Scale Inhib.* **2021**, 10 (2), 634–648. doi: 10.17675/2305-6894-2021-10-2-10
31. A. Alamiery, W. Isahak, H. Aljibori, H. Al-Asadi, A. Kadhum, Effect of the structure, immersion time and temperature on the corrosion inhibition of 4-pyrrol-1-yl-N--(2,5-dimethyl-pyrrol-1-yl)benzoylamine in 1.0 M HCl solution, *Int. J. Corros. Scale Inhib.* **2021**, 10 (2), 700–713. doi: 10.17675/2305-6894-2021-10-2-14
32. A. Alamiery, E. Mahmoudi T. Allami, Corrosion inhibition of low-carbon steel in hydrochloric acid environment using a Schiff base derived from pyrrole: gravimetric and computational studies. *Int. J. Corros. Scale Inhib.* **2021**, 10 (2), 749–765. doi: 10.17675/2305-6894-2021-10-2-17
33. M. Athar, H. Ali, M.A. Quraishi, Corrosion inhibition of carbon steel in hydrochloric acid by organic compounds containing heteroatoms, *British Corros. J.* **2002**, 37 (2), 155–158, https://doi.org/10.1179/000705902225002376.
34. L. Guo, I.B. Obot, X. Zheng, X. Shen, Y. Qiang, S. Kaya, C. Kaya, Theoretical insight into an empirical rule about organic corrosion inhibitors containing nitrogen, oxygen, and sulfur atoms, *Appl. Surf. Sci.* **2017**, 406, 301–306. https://doi.org/10.1016/j.apsusc
35. M.J. Frisch et al. Gaussian 03, Revision B.01, Gaussian Inc., Pittsburgh, PA, **2003**.
36. T. Koopmans, Ordering of wave functions and eigen-energies to the individual electrons of an atom, *Physica* **1933**, 1, 104–113.
37. A. Al-Amiery, T. Salman, K. Alazawi, L. Shaker, A. Kadhum, M. Takriff, Quantum chemical elucidation on corrosion inhibition efficiency of Schiff base: DFT investigations supported by weight loss and SEM techniques, *Int. J. Low-Carbon Technol.* **2020**, 15, 202–209. https://doi.org/10.1093/ijlct/ctz074
38. A. Al-Amiery, L. Shaker, A. Kadhum, M. Takriff, Synthesis, characterization and gravimetric studies of novel triazole-based compound, *Int. J. Low-Carbon Technol.* **2020**, 15, 164–170. https://doi.org/10.1093/ijlct/ctz067.
39. J. Yamin, E. Sheet E, A. Al-Amiery, Statistical analysis and optimization of the corrosion inhibition efficiency of a locally made corrosion inhibitor under different operating variables using RSM, *Int. J. Corros. Scale Inhibition* **2020**, 9, 502–518. https://doi.org/10.17675/2305-6894-2020-9-2-6.
40. D. Zinad, M. Hanoon, R. Salim, S. Ibrahim, A. Al-Amiery, M. Takriff, A. Kadhum.A new synthesized coumarin-derived schiff base as a corrosion inhibitor of mild steel surface in HCl medium: Gravimetric and dft studies. *International Journal of Corrosion and Scale Inhibition* **2020**, 9, 228–243. https://doi.org/10.17675/2305-6894-2020-9-1-14
41. D. Zinad, Q. Jawad, M. Hussain, A. Mahal, L. Mohamed, A. Al-Amiery, Adsorption, temperature and corrosion inhibition studies of a coumarinderivatives corrosion inhibitor for mild steel in acidic medium: gravimetricand theoretical investigations, *Int. J. Corros. Scale Inhibition* **2020**, 9, 134–151. https://doi.org/10.17675/2305-6894-2020-9-1-8.
42. A. Alamiery, E. Mahmoudi, T. Allami, Corrosion inhibition of low-carbon steel in hydrochloric acid environment using a Schiff base derived from pyrrole: gravimetric and computational studies, *Int. J. Corros. Scale Inhibition* **2021**, 10, 749–765. https://doi.org/10.17675/2305-6894-2021-10-2-17.
43. S. B. Al-Baghdadi, A. A. Al-Amiery, A. Kadhum, M. Takriff, Computational calculations, gravimetrical, and surface morphological investigations of corrosion inhibition effect of triazole derivative on mild steel in HCl, *J. Comput.*

Theoretical Nanosci. **2020**, 17, 4797–4804. https://doi.org/10.1166/jctn.2020.9328.A.A.

44. N. K. Allam, Thermodynamic and quantum chemistry characterization of the adsorption of triazole derivatives during Muntz corrosion in acidic and neutral solutions. *Appl. Surf. Sci.* **2007**, 253, 4570−4577.
45. Q. Jawad, A. Hameed, M. Abood, A. Al-Amiery, L. Shaker, A. Kadhum, S. Takriff, Synthesis and comparative study of novel triazole derived as corrosion inhibitor of mild steel in HCl medium complemented with dft calculations, *Int. J. Corros. Scale Inhibition* **2020**, 9, 688–705. https://doi.org/10.17675/2305-6894-2020-9-2-19.
46. A.A. Al-Amiery, L.M. Shaker, A.A.H. Kadhum, M.S. Takriff, Corrosion inhibition of mild steel in strong acid environment by 4-((5,5-dimethyl-3-oxocyclohex-1-en-1-yl)amino) benzenesulfonamide, *Tribol. Ind.* **2020**, 42, 89–101.
47. S. Junaedi, A. Al-Amiery, A. Kadihum, A. Kadhum, A. Mohamad, Inhibitioneffects of a synthesized novel 4-aminoantipyrine derivative on the corrosion of mild steel in hydrochloric acid solution together with quantum chemicalstudies, *Int. J. Mol. Sci.* **2013**, 14, 11915–11928. https://doi.org/10.3390/ijms140611915.
48. A. Alamiery, W.N.R.W. Isahak, H.S.S. Aljibori, H. A. Al-Asadi, A. A. H. Kadhum, Effect of the structure, immersion time and temperature on the corrosion inhibition of 4-pyrrol-1-yl-n-(2,5-dimethyl-pyrrol-1-yl)benzoylamine in 1.0 m hcl solution, *International Journal of Corrosion and Scale Inhibition* **2021**, 10, 700-713,
49. S. Al-Baghdadi, F. Hashim, A. Salam, T. Abed, T. Gaaz, A. Al-Amiery, A.H.Kadhum, K. Reda, W. Ahmed, Synthesis and corrosion inhibition application ofNATN on mild steel surface in acidic media complemented with DFT studies, *Results Phys.* **2018**, 8, 1178–1184. https://doi.org/10.1016/j.rinp.2018.02.007.
50. A. Alamiery, Anticorrosion effect of thiosemicarbazide derivative on mild steel in 1 mol L-1 hydrochloric acid and 0.5 M sulfuric acid: Gravimetrical and theoretical studies, *Materials Science for Energy Technologies* **2021**, 4, 263-273. https://doi.org/10.1016/j.mset.2021.07.004.
51. G. Gece and S. Bilgiç, Quantum chemical study of some cyclic nitrogen compounds as corrosion inhibitors of steel in NaCl media *Corrosion Science* **2009**, 51 (8), 1876–1878.
52. M. Bouklah, H. Harek, R. Touzani, B. Hammouti, and Y. Harek, DFT and quantum chemical investigation of molecular properties of substituted pyrrolidinones, *Arabian Journal of Chemistry* **2012**, 5, 163–166, 2012.
53. V. S. Sastri and J. R. Perumareddi, Molecular orbital theoretical studies of some organic corrosion inhibitors, *Corrosion* **1997**, 53, 617–622.
54. I. Lukovits, E. Kálmán, and F. Zucchi, Corrosion inhibitors–correlation between electronic structure and efficiency, *Corrosion* **2001**, 57, 3–8.